Journal of Luminescence 140 (2013) 82–86

Contents lists available at SciVerse ScienceDirect

Journal of Luminescence

journal homepage: www.elsevier.com/locate/jlumin

Photo-, radio- and thermoluminescence of Sm^{3+} doped and Tb^{3+}/Sm^{3+} doubly doped K_2YF_5 single crystals

J. Marcazzó [a,b,*], M. Santiago [a,b], V.N. Makhov [c], Vu Phi Tuyen [d], N.M. Khaidukov [e], E. Caselli [a,f]

[a] Instituto de Física Arroyo Seco-UNICEN, Pinto 399, 7000 Tandil, Argentina
[b] Consejo Nacional de Investigaciones Científicas y Técnicas (CONICET), Rivadavia 1917, 1033 Buenos Aires, Argentina
[c] Lebedev Physical Institute, RAS, Leninskii Prospekt 53, 119991 Moscow, Russia
[d] Institute of Materials Science, VAST, Hanoi, Vietnam
[e] Kurnakov Institute of General and Inorganic Chemistry, RAS, Leninskii Prospekt 31, 119991 Moscow, Russia
[f] Comisión de Investigaciones Científicas de la Provincia de Buenos Aires, calle 526 entre 10 y 11, 1900 La Plata, Argentina

ARTICLE INFO

Article history:
Received 26 September 2012
Received in revised form
27 February 2013
Accepted 5 March 2013
Available online 15 March 2013

Keywords:
Rare-earth doped K_2YF_5
Photoluminescence
Radioluminescence
Thermoluminescence

ABSTRACT

Photoluminescence, radioluminescence and thermoluminescence properties of K_2YF_5 crystals containing different concentrations of samarium and terbium ions have been investigated for the first time. It has been found that the emission peaks observed in ranges from 300 to 550 nm and from 550 to 750 nm can be attributed to the *4f–4f* transitions of the Tb^{3+} ions and the Sm^{3+} ions, respectively, for both photoluminescence and radioluminescence. The maximum of light output for radioluminescence under beta irradiation has been obtained for K_2YF_5 crystals doped with 1.0 at% Sm^{3+} ions and the prospects for using such dosimeters in fiber optic dosimetry have been evaluated. On the other hand, it has been found that the glow curves of doubly doped fluoride crystals are made up of at least four overlapping glow peaks and that K_2YF_5:1.0 at% Tb^{3+}; 0.5 at% Sm^{3+} crystals show the most intense thermoluminescence emission.

1. Introduction

Fluoride crystals have a number of interesting properties from the viewpoint of both basic research and technological applications. Some favorable physical properties of fluoride compounds are high transparency in a wide range of wavelengths from vacuum ultraviolet to infrared regions and high radiation stability in comparison with other halogen crystals [1]. Besides, fluoride crystals doped with optically active rare earth ions exhibit efficient luminescence. In particular, doped K_2YF_5 crystals have been widely studied during past years and it has been discovered that luminescence materials based on this fluoride compound containing different concentrations of Ce^{3+}, Pr^{3+}, Tb^{3+} and Dy^{3+} ions seem to be promising detectors for thermoluminescence (TL) dosimetry from the viewpoint of both detecting and discriminating between components of mixed radiation fields [2–5].

On the other hand, Tb^{3+} or Sm^{3+} doped fluoride crystals show very attractive radioluminescence (RL) properties. For example, Tb^{3+} doped CsY_2F_7 and $CsGd_2F_7$ crystals possess efficient radioluminescence characteristics and there are no changes in their RL responses as a function of the accumulated dose under irradiation, which makes these Tb^{3+} doped crystals promising for RL dosimetry [6]. There is also a high long-term stability of RL response under irradiation for Sm^{3+} doped crystals and most part of RL emission from Sm^{3+} ions is realized at wavelengths longer than 550 nm whereas the Cerenkov emission is almost negligible in this part of the spectral range. These characteristics are very useful for using such materials in fiber-optic RL dosimetry [7,8]. It should also be noted that some rare earth ions, for example Ce^{3+} and Tb^{3+}, incorporated into crystal lattices always act as hole traps whereas other rare earth ions, for example Sm^{3+} and Eu^{3+}, act as electron traps, and rare earth ions of these types can be simultaneously recombination and luminescent centers [3]. Perhaps, in some cases, the materials doubly doped with rare earth ions of different types will show non-additive properties in comparison with singly doped materials. In particular, doubly rare earth doped compounds are used as long lasting afterglow phosphors for different applications [9].

Within this research K_2YF_5 crystals doped with Sm^{3+} and co-doped with Tb^{3+} have been synthesized under hydrothermal conditions and their photoluminescence, radioluminescence and thermoluminescence have been examined as a function of the rare earth concentrations. Also, the feasibility of using these crystals as radiation dosimeters has been evaluated.

2. Experimental

Crystals of orthorhombic K_2YF_5 fluoride doped with optically active rare earth ions were grown under hydrothermal conditions.

* Corresponding author at: Instituto de Física Arroyo Seco-UNICEN, Pinto 399, 7000 Tandil, Argentina. Tel.: +54 249 4439660.
E-mail address: jmarcass@exa.unicen.edu.ar (J. Marcazzó).
URL: http://ifas.exa.unicen.edu.ar (J. Marcazzó).

0022-2313/$ - see front matter © 2013 Elsevier B.V. All rights reserved.
http://dx.doi.org/10.1016/j.jlumin.2013.03.009

For hydrothermal experiments, copper insert lined autoclaves having a volume of about 40 cm^3 were utilized and the inserts were separated into synthesis and crystallization zones by perforated diaphragms. The fluoride crystals were synthesized by a direct temperature-gradient method as a result of the reaction of the aqueous solutions containing 40–50 mol% KF with oxide mixtures $(1-x-y)\,Y_2O_3 - x\,Sm_2O_3 - y\,Yb_2O_3$ at a temperature of about 750 K in the synthesis zone, a temperature gradient along the reactor body of up to 3 K cm^{-1}, and a pressure of about 100 MPa. Under these conditions, spontaneously nucleated crystals up to 0.5 cm^3 in size were grown in the upper crystallization zone of the autoclave for 200 h [10]. The structure type and phase purity of synthesized samples were characterized by powder X-ray diffraction and the purities of the utilized oxides were 99.99%. In order to compare the RL efficiency of these fluorides with a commercial RL dosimeter, Landauer Inc. manufactured Al_2O_3:C discs of 5 mm in diameter and 0.9 mm in thickness were used. Here it should be mentioned that Al_2O_3:C is one of the standard materials for fiber-optic RL dosimetry [11].

The photoluminescence and excitation spectra were measured using synchrotron radiation from the DORIS storage ring at the Superlumi station [12] of HASYLAB at DESY (Hamburg, Germany). Emission spectra in the spectral range 350–740 nm were recorded with a 0.3-m Czerny–Turner monochromator-spectrograph SpectraPro-308i (Acton Research Inc.) with a liquid nitrogen cooled CCD detector (Princeton Instruments Inc.). The same spectrograph with a R6358P (Hamamatsu) photomultiplier tube (PMT) was applied for selecting the monitored wavelength when measuring excitation spectra in the range 50–220 nm. Excitation spectra were recorded with spectral resolution ~0.3 nm, and emission spectra ~0.5 nm. The samples (small single crystals with the size less than 1 mm) were grounded into powders and mounted into small copper cups (with a diameter of 3 mm and thickness of 1 mm), which were then glued onto a copper sample holder of a flow-type liquid helium cryostat. All measurements have been performed under ultrahigh vacuum conditions.

Radioluminescence curves were measured as a function of time during beta irradiation. All the samples were irradiated at RT with a 10 mCi ophthalmic ^{90}Sr beta-source rendering a dose rate of 0.024 Gy min^{-1} at the sample position. The light emitted by the samples was collected by means of a ϕ1 mm communication grade optical fiber and projected onto a Hamamatsu H9319 photon counting PMT having sensitivity between 300 and 850 nm. Radioluminescence spectra were recorded in the wavelength range 300–800 nm at a rate of 10 nm min^{-1} by means of an Acton Research SP-2155 0.150 meter monochromator featuring the same photon counting PMT. The sample was placed at the entrance slit and irradiated with the beta source, which was situated 1 cm away from the sample. Both the entrance and exit slits were set to a width of 3 mm during the measurements, which result in a resolution of approximately 10 nm.

For measuring the thermoluminescence glow curves, a Harshaw-Bicron 3500 TL reader featuring a Hamamatsu R6094 photomultiplier tube was used and the samples were heated from room temperature (RT) up to 375 °C with a constant heating rate of 1.0 °C s^{-1}. In order to empty the active traps completely, an annealing of the samples at 375 °C for 1 min was performed inside the same TL reader before irradiation.

3. Results and discussion

3.1. Photoluminescence

Fig. 1 shows low-temperature (7.0 K) luminescence spectra of Sm^{3+} singly doped and Tb^{3+}/Sm^{3+} doubly doped K_2YF_5 crystals in the range from 350 to 740 nm under vacuum ultraviolet (VUV) excitation.

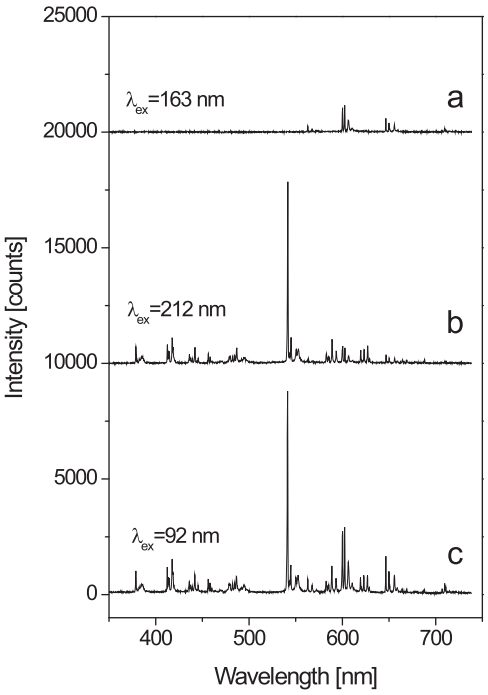

Fig. 1. Emission spectra of K_2YF_5:1.0 at% Sm^{3+} under 163 nm excitation (a) and K_2YF_5:1.0 at% Tb^{3+}; 1.0 at% Sm^{3+} under 212 nm (b) and 92 nm (c) excitation. The detailed assignment of the different emission lines to Tb^{3+} and Sm^{3+} can be found in the text.

The luminescence spectrum of K_2YF_5:1.0 at% Sm^{3+} under 163 nm excitation (curve (a)) shows typical samarium emission with four groups of lines at 560, 600, 650 and 710 nm corresponding to Sm^{3+} 4*f*–4*f* multiplet transitions: $^4G_{5/2}\rightarrow{}^6H_J$ ($J=5/2,7/2,9/2,11/2$), respectively [8,14,15]. The number of lines for transitions to each *J*-multiplet exactly corresponds to the number of Stark components ($(2J+1)/2$) of the corresponding terminal multiplet term. Curves (b) and (c) show luminescence spectra of K_2YF_5:1.0 at% Tb^{3+}; 1.0 at% Sm^{3+} under 212 and 92 nm excitation, respectively. In these curves, in addition to the aforementioned lines of Sm^{3+} transitions, several other groups of lines corresponding to Tb^{3+} transitions are observed. In particular, the lines grouped at 380, 415, 435 and 460 nm are related to the $^5D_3\rightarrow{}^7F_J$ Tb^{3+} transitions ($J=6,5,4,3$), respectively [16–18]. The groups of lines observed at 480, 540, 580 and 620 nm are related to the $^5D_4\rightarrow{}^7F_J$ Tb^{3+} transitions ($J=6,5,4,3$) , respectively [6,16].

The low-temperature (7.0 K) excitation spectrum of Sm^{3+} 4*f*–4*f* emission from K_2YF_5:Sm^{3+} at 603 nm (Fig. 2, curve (a)) is dominated by the broad band with the onset at ~170 nm corresponding to the lowest energy 4*f*–5*d* transition of Sm^{3+}. The transitions to higher energy 5*d* crystal-field levels of Sm^{3+} are observed in the range of 150–115 nm, which are probably overlapped at $\lambda\leq135$ nm with F^-–Sm^{3+} charge-transfer transitions. The host related excitation occurs at wavelengths below 115 nm. In the excitation spectrum of Sm^{3+} emission from K_2YF_5 doubly doped with Sm^{3+} and Tb^{3+} at 603 nm (Fig. 2, curve (b)) the same broad band with the onset at ~170 nm corresponding to the lowest energy 4*f*–5*d* transition of Sm^{3+} dominates. However, in this spectrum an additional broad band with the longer wavelength onset at ~217 nm appears, which corresponds to the lowest energy 4*f*–5*d* transition of Tb^{3+}. This can be well seen by comparing this spectrum with excitation spectrum of Tb^{3+} emission at ~541.2 nm (Fig. 2, curve (c)).

Thus, in K_2YF_5 doubly doped with Sm^{3+} and Tb^{3+} an efficient energy transfer from Tb^{3+} to Sm^{3+} is observed for concentrations of the dopant ions ~1.0 at%, i.e. in such system the Tb^{3+} ion serves as a sensitizer ion for Sm^{3+} luminescence, the photon energy for

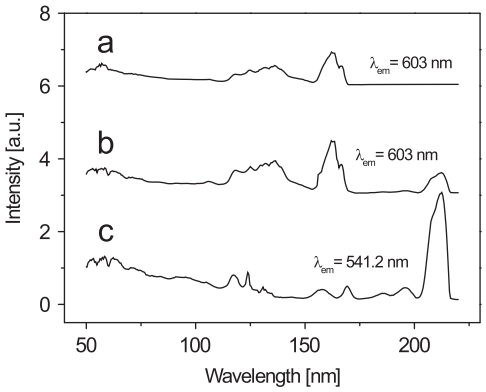

Fig. 2. Excitation spectra of K_2YF_5:1.0 at% Sm^{3+} monitoring Sm^{3+} luminescence at 603 nm (a) and of K_2YF_5:1.0 at% Tb^{3+}; 1.0 at% Sm^{3+} monitoring Sm^{3+} luminescence at 603 nm (b) and Tb^{3+} luminescence at 541.2 nm (c).

efficient excitation of Sm^{3+} emission being lower than in the case of the crystal singly doped with Sm^{3+}. The energy transfer from Tb^{3+} to Sm^{3+} can also be recognized from the luminescence spectrum of K_2YF_5:1.0 at% Tb^{3+}; 1.0 at% Sm^{3+} presented in Fig. 1 where two groups of lines from both Tb^{3+} and Sm^{3+} are observed under Tb^{3+} 4*f*–5*d* excitation at 212 nm.

One can think that the reversed energy transfer from Sm^{3+} to Tb^{3+} can also be realized in the studied system. However, it is clearly seen from Fig. 2 that the excitation spectrum of Tb^{3+} emission at 541.2 nm from K_2YF_5:1.0 at% Tb^{3+}; 1.0 at% Sm^{3+} in the region of efficient absorption by Sm^{3+} (in the range 115–170 nm) has different shapes than excitation spectrum of Sm^{3+} emission at 603 nm. In this excitation region the latter spectrum is practically identical to excitation spectrum of Sm^{3+} emission from K_2YF_5 singly doped with Sm^{3+}. This indicates that under Sm^{3+} absorption mainly Sm^{3+} emission is excited in K_2YF_5:1.0 at% Tb^{3+}; 1.0 at % Sm^{3+} without significant energy transfer to Tb^{3+}.

The mechanism of the energy transfer from Tb^{3+} to Sm^{3+} can be represented as follows. After the Tb^{3+} ion is excited by VUV photon into its 4*f*–5*d* electronic configuration the fast nonradiative relaxation occurs in the Tb^{3+} emitting $^5D_3$ and $^5D_4$ 4*f* levels. Then the energy from these Tb^{3+} levels is transferred nonradiatively to the excited Sm^{3+} 4*f* levels with similar energy due to the direct energy transfer. After that the nonradiative relaxation takes place within Sm^{3+} ion to its emitting 4*f* level $^4G_{5/2}$. The back energy transfer from Sm^{3+} to Tb^{3+} is very unprobable because the emitting level $^4G_{5/2}$ of Sm^{3+} is located about 2600 cm^{-1} below the lowest Tb^{3+} emitting level $^5D_4$.

Definitely, the studies of Tb^{3+}/Sm^{3+} doubly doped K_2YF_5 systems with varying concentrations of the doping ions are needed for the determination of optimal concentrations of Tb^{3+} and Sm^{3+} for mostly efficient energy transfer.

3.2. Radioluminescence

Fig. 3 shows the curves of the RL intensity from K_2YF_5 crystals doped with different Sm^{3+} concentrations under beta irradiation at RT as a function of time. In the same figure, the intensity of RL emission from Al_2O_3:C is shown for comparison. All the RL curves have been normalized to the sample weight. Among the Sm^{3+} doped crystals, K_2YF_5:1.0 at% Sm^{3+} has the most intense RL emission. The curves of the RL intensity from K_2YF_5 crystals doubly doped with Sm^{3+} and Tb^{3+} at RT are shown in Fig. 4. Among these crystals, K_2YF_5:1.0 at% Tb^{3+}; 1.0 at% Sm^{3+} shows the highest RL intensity. The doubly doped fluorides present a stable signal reaching the maximum intensity immediately after irradiation in contrast to the compositions singly doped with Sm^{3+} for which the maximum of the RL intensity is reached after 50 s of irradiation. It is apparent from Figs. 3 and 4 that

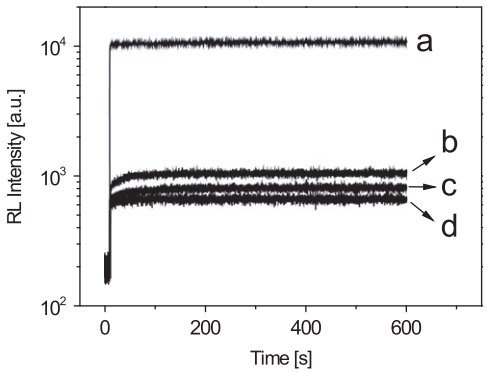

Fig. 3. RL light yield of Al_2O_3:C (a), K_2YF_5:1.0 at% Sm^{3+} (b), K_2YF_5:2.0 at% Sm^{3+} (c) and K_2YF_5:0.5 at% Sm^{3+} (d).

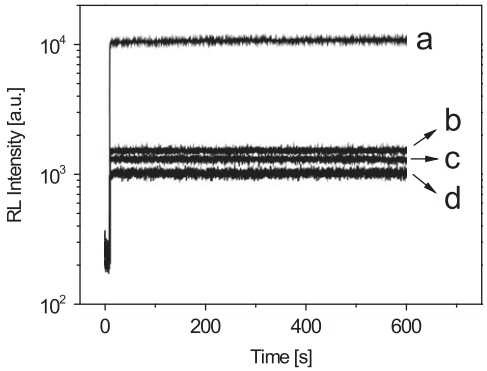

Fig. 4. RL light yield of Al_2O_3:C (a), K_2YF_5:1.0 at% Tb^{3+}; 1.0 at% Sm^{3+} (b), K_2YF_5:1.0 at% Tb^{3+}; 2.0 at% Sm^{3+} (c) and K_2YF_5:1.0 at% Tb^{3+}; 0.5 at% Sm^{3+} (d).

the RL light yield from the studied samples is roughly one order of magnitude less than that of a commercial Al_2O_3:C detector.

Fig. 5 shows the RL spectra of Al_2O_3:C, K_2YF_5:1.0 at% Sm^{3+} and K_2YF_5:1.0 at% Tb^{3+}; 1.0 at% Sm^{3+} under beta irradiation. Al_2O_3:C has a broad emission band between 370 and 500 nm with a maximum at 420 nm as expected [13]. On the other hand, in the spectrum of K_2YF_5:1.0 at% Sm^{3+} there are four bands at 560, 600, 650 and 710 nm which, as mentioned above, can be attributed to aforementioned 4*f*–4*f* transitions in Sm^{3+} [8,14,15]. As for K_2YF_5:1.0 at% Tb^{3+}; 1.0 at% Sm^{3+}, in its RL spectra there are bands at 380, 415, 480, 550, 600, 650, 710 and 760 nm having different intensities. The first four bands, as mentioned above, can be attributed to the 4*f*–4*f* Tb^{3+} transitions [6,16]. The bands at 600, 650 and 710 nm can also be attributed to the aforementioned Sm^{3+} transitions. In other words, RL spectra of both K_2YF_5:1.0 at% Sm^{3+} and K2YF5:1.0 at% Tb^{3+}; 1.0 at% Sm^{3+} are in agreement with the PL emission spectra as shown in Fig. 1.

From the viewpoint of using these fluorides in fiber-optic dosimetry (FOD) both K_2YF_5: 1.0 at% Sm^{3+} and K_2YF_5: 1.0 at% Tb^{3+}; 1.0 at% Sm^{3+} have the advantage in comparison with Al_2O_3:C as they have luminescence above 550 nm, where the Cherenkov emission usually found in FOD is almost negligible [19]. In fact, if the RL intensity of these samples is filtered by means of a long pass filter with cut-off wavelength at 570 nm most of their RL signal can be collected while avoiding the mainly blue contribution of Cherenkov emission. In this context, the possibility of using these fluorides in FOD technique is worth for further consideration.

3.3. Thermoluminescence

The TL glow curves of Sm^{3+} doped and Sm^{3+}/Tb^{3+} doubly doped K_2YF_5 crystals are shown in Figs. 6 and 7, respectively. It is evident from Fig. 6 that among the Sm^{3+} doped crystals, K_2YF_5:0.5 at% Sm^{3+} has the highest TL response to beta radiation.

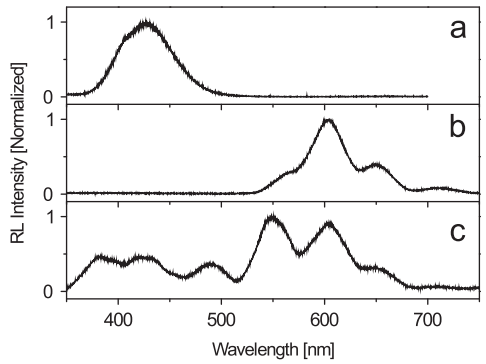

Fig. 5. RL spectra of Al_2O_3:C (a), K_2YF_5:1.0 at% Sm^{3+} (b) and K_2YF_5:1.0 at% Tb^{3+}; 1.0 at% Sm^{3+} (c).

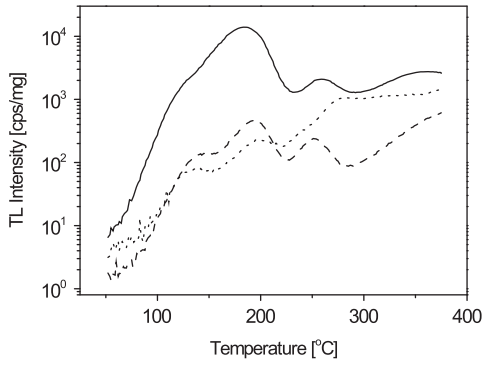

Fig. 6. TL glow curves of K_2YF_5:0.5 at% Sm^{3+} (solid curve), K_2YF_5:1.0 at% Sm^{3+} (dashed curve) and K_2YF_5:2.0 at% Sm^{3+} (dotted curve).

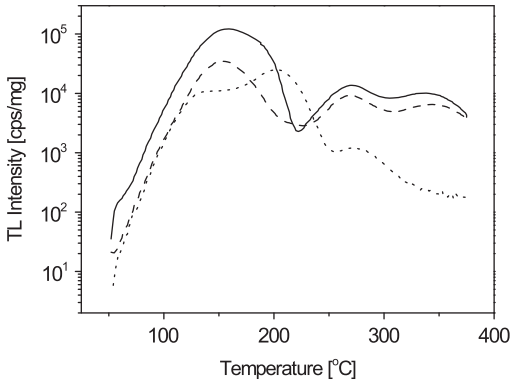

Fig. 7. TL glow curves of K_2YF_5:1.0 at% Tb^{3+}; 0.5 at% Sm^{3+} (solid curve), K_2YF_5:1.0 at% Tb^{3+}; 1.0 at% Sm^{3+} (dashed curve) and K_2YF_5:1.0 at% Tb^{3+}; 2.0 at% Sm^{3+} (dotted curve).

The integrated TL intensity for this composition is more than one order of magnitude higher than that from any of the Sm^{3+} doped fluorides investigated in this work. On the other hand, among the crystals doubly doped with Sm^{3+} and Tb^{3+}, K_2YF_5:0.5 at% Sm^{3+}; 1.0 at% Tb^{3+} presents the most intense TL response. In fact, its TL intensity is three and five times higher than those of K_2YF_5:1.0 at% Sm^{3+}; 1.0 at% Tb^{3+} and K_2YF_5:2.0 at% Sm^{3+}; 1.0 at% Tb^{3+}, respectively. It is apparent from these results that within the investigated range of doping concentrations the TL response of K_2YF_5 fluorides increases when the Sm^{3+} concentration decreases. In order to evaluate the feasibility of using the most efficient compound as TL dosimeter the response of K_2YF_5:0.5 at% Sm^{3+}; 1.0 at% Tb^{3+} as a function of the dose has been measured. In Fig. 8 the area under the most intense glow peak (50–220 °C) of K_2YF_5:0.5 at% Sm^{3+}; 1.0 at% Tb^{3+} is shown. A linear regression performed on the experimental data has rendered a regression coefficient equal to 0.999, which demonstrates a very acceptable linear response.

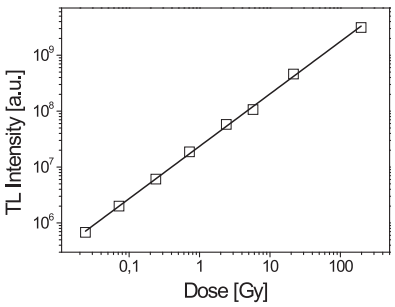

Fig. 8. Dose response of K_2YF_5:1.0 at% Tb^{3+}; 0.5 at% Sm^{3+} between 0.01 and 200 Gy. The solid line is a linear fit included for the eye guide.

4. Conclusion

A series of K_2YF_5 crystals doped with Sm^{3+} and doubly doped with Sm^{3+} and Tb^{3+} with different concentrations of the dopants have been successfully synthesized under hydrothermal conditions. The synthesized crystals show well-recognized characteristic 4*f*–4*f* luminescence of the Tb^{3+} and Sm^{3+} ions, mostly at wavelengths longer than 550 nm, under both photoexcitation and beta irradiation. The TL glow curves of these crystals after beta irradiation have rather complicated shape with at least four overlapping glow peaks and the intensity of the TL response strongly depends on the concentration of the doping ions. Although intensities of RL and TL among synthesized crystals have been examined as a function of dopant concentrations it is obvious that additional investigations are needed in order to find the optimal concentrations of Sm^{3+} and Tb^{3+} under which the highest efficiencies of RL and TL can be reached. Anyway, the performed studies have shown that Sm^{3+} doped and Sm^{3+}/Tb^{3+} doubly doped K_2YF_5 crystals are promising detector materials for applications in FOD and TL dosimetry.

Acknowledgments

This research has been supported by the Vietnam's National Foundation for Science and Technology Development (NAFOSTED) with project code 103.06.44.09 and the Russian Foundation for Basic Research (RFBR project 10-03-90305) as well as the Agencia Nacional de Promoción Científica y Tecnológica (ANPCyT, Argentina, Grant PICT Red 1907) and the Consejo Nacional de Investigaciones Científicas y Técnicas (CONICET, Argentina, Grant PIP 241). The authors acknowledge Dr. Aleksei Kotlov, station scientist at DESY/HASYLAB, for his assistance in the photoluminescence measurements.

References

[1] Min Yin, J.C. Krupa, E. Antic Fidancev, V.N. Makhov, N.M. Khaidukov, J. Lumin. 101 (2003) 79.
[2] J. Marcazzo, M. Santiago, E. Caselli, N. Nariyama, N.M. Khaidukov, Opt. Mater. 26 (2004) 65.
[3] H.W. Kui, D. Lo, Y.C. Tsang, N.M. Khaidukov, V.N. Makhov, J. Lumin. 117 (2006) 29.
[4] E.C. Silva, N.M. Khaidukov, M.S. Nogueira, L.O. Faria, Radiat. Meas. 42 (2007) 311.
[5] H.K. Hanh, N.M. Khaidukov, V.N. Makhov, V.X. Quang, N.T. Thanh, V.P. Tuyen, Nucl. Instrum. Methods Phys. Res. B 268 (2010) 3344.
[6] J. Marcazzó, J. Henniger, N.M. Khaidukov, V.N. Makhov, E. Caselli, M. Santiago, J. Phys. D: Appl. Phys. 40 (2007) 5055.

[7] C.J. Marckmann, M.C. Aznar, C.E. Andersen, L. Bøtter-Jensen, R. Gaza, S.W. S. McKeever, Radiat. Prot. Dosimetry 119 (2006) 363.
[8] J. Marcazzó, M. Santiago, C. DÁngelo, C. Furetta, E. Caselli, Nucl. Instrum. Methods Phys. Res. B 268 (2010) 183.
[9] Y. Liu, J. Kuang, B. Lei, C. Shi, J. Mater. Chem. 15 (2005) 4025.
[10] M.A. Dubinskii, N.M. Khaidukov, I.G. Garipov, L.N. Dem'yanets, A.K. Naumov, V. V. Semashko, V.A. Malyusov, J. Mod. Opt. 37 (1990) 1355.
[11] C.E. Andersen, S.K. Nielsen, S. Greilich, J. Helt-Hansen, Med. Phys. 36 (2009) 708.
[12] G. Zimmerer, Radiat. Meas. 42 (2007) 859.
[13] G. Erfurt, M.R. Krbetschek, Radiat. Prot. Dosimetry 100 (2002) 403.
[14] A. Thulasiramudu, S. Buddhudu, Spectrochim. Acta A 67 (2007) 802.
[15] B.H. Rudramadevi, S. Buddhudu, Indian J. Pure Appl. Phys. 46 (2008) 825.
[16] A.J.J. Bos, M. Prokic, J.C. Brouwer, Radiat. Prot. Dosimetry 119 (2006) 130.
[17] Z. Lin, X. Liang, Y. Ou, C. Fan, S. Yuan, H. Zeng, G. Chen, J. Alloys Compd. 496 (2010) L33.
[18] C. Zhu, X. Liang, Y. Yang, G. Chen, J. Lumin. 130 (2010) 74.
[19] L. Archambault, A.S. Beddar, L. Gingras, R. Roy, L. Beaulieu, Med. Phys. 33 (2006) 128.